Intermetallics 18 (2010) 2468–2471

Contents lists available at ScienceDirect

Intermetallics

journal homepage: www.elsevier.com/locate/intermet

Short communication

Fractal in fracture of bulk metallic glass

M.Q. Jiang [a,b], J.X. Meng [a], J.B. Gao [c], X.-L. Wang [d], T. Rouxel [e], V. Keryvin [e], Z. Ling [a], L.H. Dai [a,b,*]

[a] State key Laboratory of Nonlinear Mechanics, Institute of Mechanics, Chinese Academy of Sciences, No 15 Beisihuan Road, Beijing 100190, People's Republic of China
[b] State Key Laboratory of Explosion Science and Technology, Beijing Institute of Technology, Beijing 100081, People's Republic of China
[c] PMB Intelligence LLC, P.O. Box 2077, West Lafayette, IN 47996, USA
[d] Neutron Scattering Science Division, Oak Ridge National Laboratory, Oak Ridge, TN 37831, USA
[e] Applied Mechanics Laboratory of the University of Rennes 1, LARMAUR, ERL CNRS 6274, Université de Rennes 1, Campus de Beaulieu, 35042 Rennes cedex, France

ARTICLE INFO

Article history:
Received 4 July 2010
Accepted 1 August 2010
Available online 9 September 2010

Keywords:
A. Bulk metallic glass
B. Dynamic fracture
C. Nanoscale periodic corrugation
C. Fractal

ABSTRACT

We investigate the nanoscale periodic corrugation (NPC) structures on the dynamic fracture surface of a typical tough bulk metallic glass, submitted to high-velocity plate impact and scanned by atomic force microscopy (AFM). The detrended fluctuation analysis (DFA) of the recorded AFM profiles reveals that the valley landscapes of the NPC are nearly memoryless, characterized by Hurst parameter of 0.52 and exhibiting a self-similar fractal character with the dimension of about 1.48. Our findings confirm the existence of the "quasi-cleavage" fracture underpinned by tension transformation zones (TTZs) in metallic glasses.

1. Introduction

In crystalline metals, atomic bonds are particularly susceptible to rupture in shear (slip) and tension (cleavage) across preferred crystallographic planes, leading to ductile and brittle fracture, respectively. Unlike long-range slip in crystals, the ductile fracture of glassy metals is guided by the nanoscale shear banding ahead of the crack [1–5], where the blunt tip advances via continuous operations of "flow defect" [6] or "shear transformation zone" (STZ) [7]. The STZ is essentially a local atomic cluster that undergoes an inelastic shear distortion from one relatively low local energy basin to a second, crossing an activated configuration of higher energy and volume [8–10]. The ductile crack propagation can leave cell or river-like vein patterns on final fracture surfaces [11–13], due to the fluid meniscus instability [1,2] initially discussed by Taylor [14]. Recently, however, a new pattern – the nanoscale periodic corrugation (NPC), has been widely observed in various metallic glasses (MGs) covering ideally brittle Mg-based [15–19], Fe-based [17,19], Co-based [17], and rare earth-based [19], less brittle Ni-based [20] and even tough Zr-based [21–25], indicating its universality. The characteristic size, i.e. the spacing of NPC is usually smaller than the critical wavelength of the fluid meniscus instability [16,18,21]. This poses a big challenge to the STZ-mediated ductile fracture mechanism.

Based on a broad overview of fracture patterns [21,22,26], we have previously proposed that the NPC forms via periodically activation of tension transformation zones (TTZs) with local plastic flow in the background ahead of the crack tip. The TTZ can be envisioned as a transient transition from a STZ that experiences significant tension/dilatation fracture [21,24,26]. Compared to a STZ being the elementary process of ductile cracking, a TTZ can be regarded as the basis of brittle "quasi-cleavage" fracture through which energy dissipates mainly by forming new surfaces and little by accompanying weaker plastic flow. The fracture mechanism via STZ versus TTZ is of paramount importance in understanding the ductile-to-brittle transition in MGs [21,24–26]. The STZ-underpinned ductile fracture plane has been widely studied [1,2,11–13], but a quantitative analysis on the TTZs-mediated "quasi-cleavage" surface is not yet available. Therefore, in this paper, we perform an exhaustive investigation of the NPC in a typical Zr-based bulk MG by atomic force microscopy (AFM). A detrended fluctuation analysis (DFA) method is adopted to quantitatively analyze the AFM topographical profiles recorded, which allowed us to identify our proposed "quasi-cleavage" fracture mechanism on the basis of TTZs in metallic glasses.

2. Experimental observations

Fig. 1a is a high-resolution scanning electron microscope (HRSEM) image of representative NPC that has been observed on

* Corresponding author at: State key Laboratory of Nonlinear Mechanics, Institute of Mechanics, Chinese Academy of Sciences, No 15 Beisihuan Road, Beijing 100190, People's Republic of China. Tel.: +86 10 82543958; fax: +86 10 82543977.
E-mail address: lhdai@lnm.imech.ac.cn (L.H. Dai).

0966-9795/$ – see front matter © 2010 Elsevier Ltd. All rights reserved.
doi:10.1016/j.intermet.2010.08.003

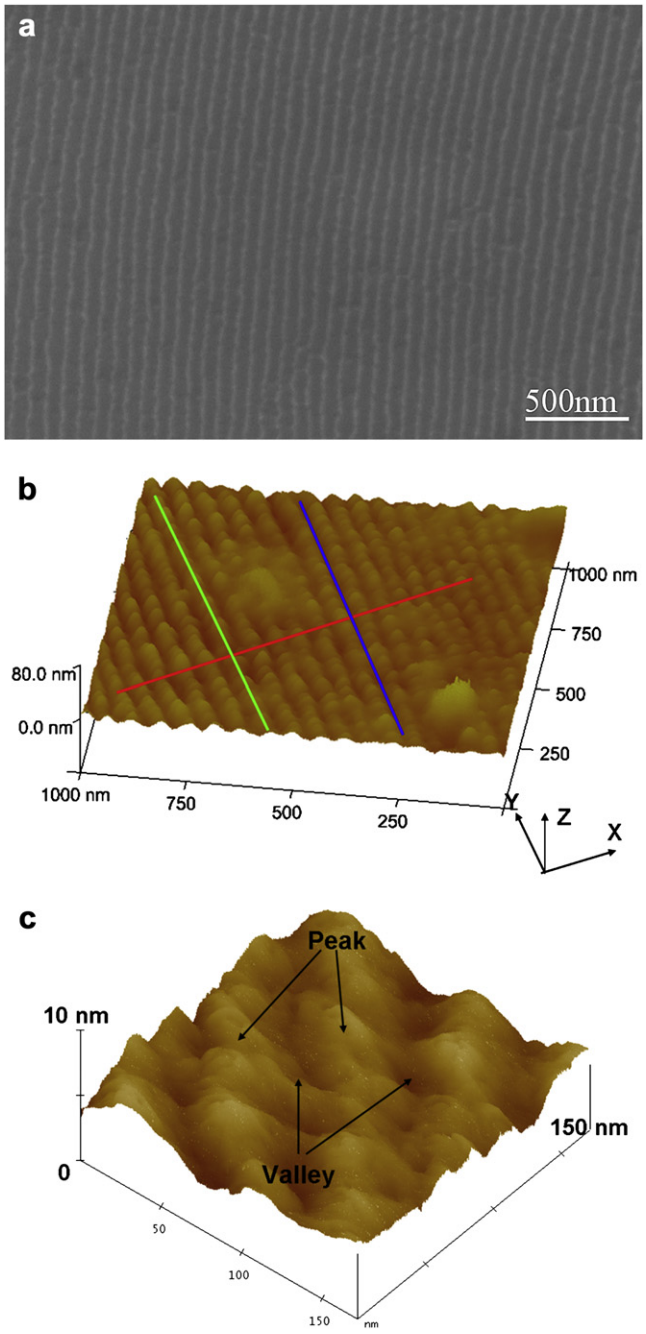

Fig. 1. Nanoscale periodic corrugation (NPC) observed on dynamic facture surface of Vit 1 bulk MGs under high-velocity impact. (a) HRSEM image of the NPC. (b) and (c) AFM 3D image of a NPC at different magnification. [For interpretation of the references to color in this figure legend, the reader is referred to the web version of this article].

dynamic mode I facture planes of Vit 1 ($Zr_{41.2}Ti_{13.8}Cu_{10}Ni_{12.5}Be_{22.5}$) bulk MGs subjected to high-velocity (up to $\sim 500\ ms^{-1}$) plate impact experiments [21,22]. In order to eliminate the projection effects, we used an AFM with a spatial-resolution of 1 nm (horizontal) and 0.1 nm (vertical) to directly probe into the precise structure of the NPC. It is important to point out that the present AFM spatial-resolution (close to medium-range-order) is enough to capture the details of the NPC. Fig. 1b presents the AFM three-dimensional (3D) image (1000 nm × 1000 nm) of the NPC, in which the crack propagates along the x direction. It can be seen that the straight corrugations perpendicular to the cracking direction have approximately a regular spacing. A more magnified landscape of the NPC is shown in Fig. 1c. It is noted that the peak and valley parts (as marked in Fig. 1c) have respective fine structures with different shapes, calling for a quantitative analysis. To this end, we register 15–20 different vertical profiles of the NPC along the direction of crack propagation (the red line in Fig. 1b), the peak (the green line in Fig. 1b) and the valley (the blue line in Fig. 1b), respectively, using the AFM scans. A representative profile along the crack direction exhibits a near sinusoidal curve with the peak-to-valley alternation, as shown in Fig. 2a. The mean peak-to-peak distance is about 65 nm. The profile along the peak displays a less wavy shape (Fig. 2c) whose wavelength is not easily determined by eyes. Rather differently, the surface profile along the valley looks chaotic and has no obvious periodicity, as shown in Fig. 2e.

3. Detrended fluctuation analysis

Next we resort to a sophisticated DFA method [27] to determine the key scaling parameter, the Hurst parameter H, that permits the detection of long-range correlations embedded in the AFM topographical profiles recorded, such as Fig. 2a, c and e. The DFA method works as follows [27–29]. First divide a profile curve of length N into N/m nonoverlapping segments, each containing m data; then define the "local trend" in each segment to be the ordinate of a linear least-squares fit for the random walk displacement in that segment; finally compute the "detrended walk", denoted by $y_m(n)$, as the difference between the origin walk $y(n)$ and the local trend. Then one can examine $F_d(m) = \langle \sum_{i=1}^{m} y_m(i)^2 \rangle^{1/2} \sim m^H$, where the angular bracket denotes the ensemble average of all the segments of length m. If we plot the logarithmic $F_d(m)$ versus logarithmic m, the slope of the curve is H. A higher Hurst parameter implies stronger long-range correlated surface landscape. The DFA can also indicate the scale range where the scaling exists. Note that, if the profile is a fractal curve, its fractal dimension D_f is related to H by [28] $D_f = 2-H$, here $1 < D_f \leq 2$ for one-dimension case.

4. Results and discussion

Interestingly, we demonstrate the distinct scaling behaviors of the fracture profiles along the propagation direction, the peak and the valley, respectively, based on the DFA. Fig. 2b gives the DFA results of the AFM profiles along the propagation direction. We observe that the average $H = 1.08$ when m is not too large, and becomes very small for large m. The corresponding fractal dimension is 0.92 smaller than 1, implying the profile in Fig. 2a is *not* a fractal. The crossover point $\log_2 m = 5$ corresponds to a characteristic length scale $L_c = 64$ nm that compares well with the average spacing of the NPC (see Fig. 2a). This implies that when the observer ruler L is smaller than the characteristic length L_c, the facture surfaces along the crack direction have the strong long-range correlation. Once $L > L_c$, they show a noise at low spatial frequencies, denoting antipersistent correlation with $H << 1/2$ [27]. The DFA of profiles along the peak, as shown in Fig. 2d, also exhibits two distinct regions: at not too large length scale m the average slopes $H = 0.95$, whereas at scales larger than a crossover length $L_c = 32$ nm the tangent slopes H are significantly smaller than 1/2. It is worth noting that the critical length scale ($L_c = 32$ nm) is indeed the periodicity inherently embedded in the fracture profiles along the peak (see Fig. 2c), although these profiles look random. Within the range of $L \leq 32$ nm, the long-range correlation ($H = 0.95$) of the profiles infers that the local plastic flow occurs during the formation of peak portion of the NPC. However, this characteristic length is smaller than the wavelength (~ 85 nm) of the initial perturbation of the meniscus instability for Vit 1 bulk MGs [21,26]. According to

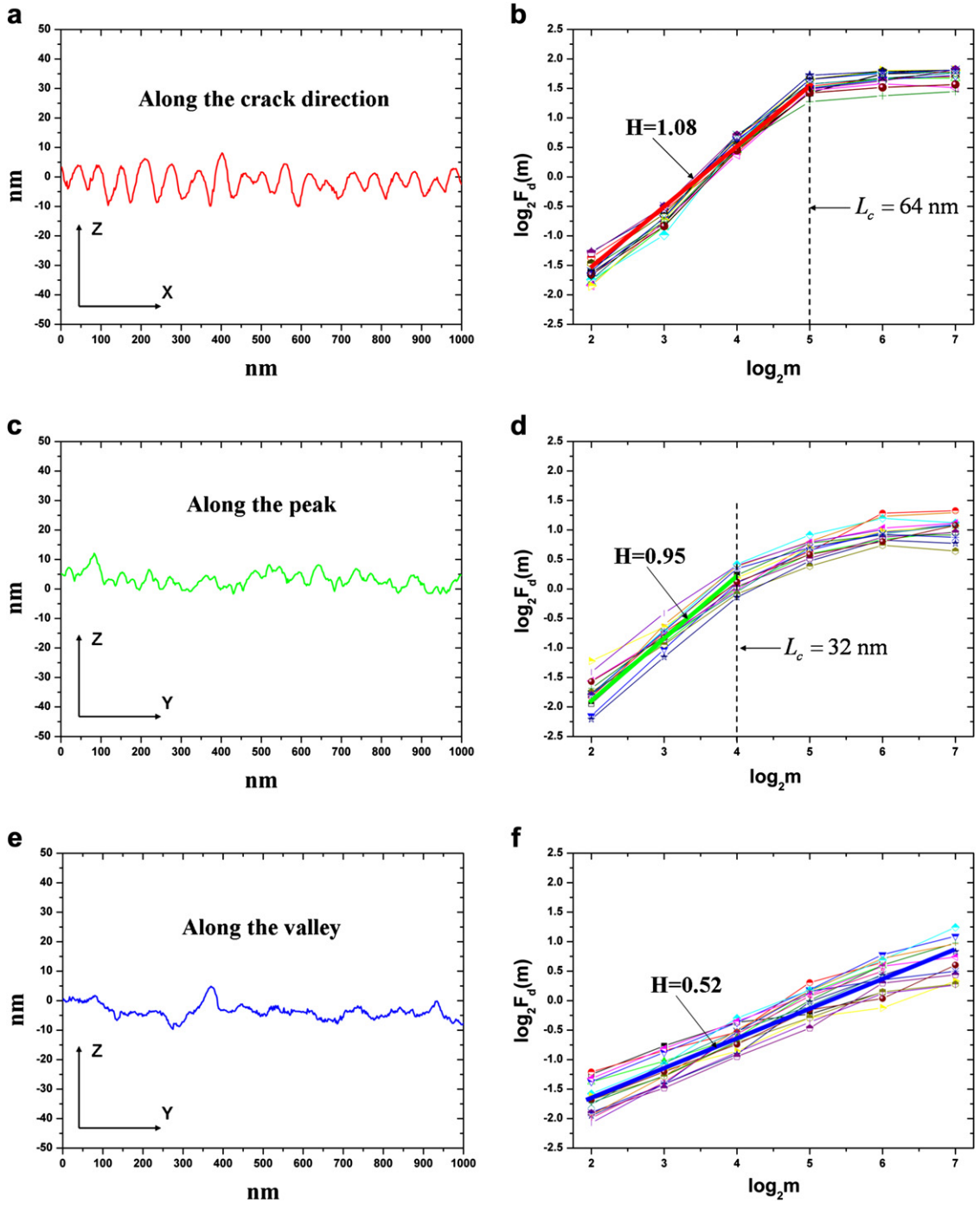

Fig. 2. Representative AFM profiles (left column) and their corresponding DFA results (right column) of NPC (a)-(b) along the crack direction, e.g. the red line in Fig. 1b, (c)-(d) along the peak, e.g. the green line in Fig. 1(b) and (e)-(f) along the valley, e.g. the blue line in Fig. 1b. [For interpretation of the references to color in this figure legend, the reader is referred to the web version of this article].

the ductile-to-brittle criterion for fracture of MGs [21,26,30], the meniscus instability actually does not develop during such extremely local flow. Moreover, with the attendant long-range correlated plastic flow in nanoscale, the peak profiles also display very *weak*-fractal character with the dimension of about 1.05. Such fractal behavior of peaks maybe arises from the effect of the neighboring valleys that are fractal (*vide post*). In the case of the profiles along the valleys (see Fig. 2e), $\log_2 F_d(m)$ is proportional to $\log_2 m$ with the mean $H = 0.52$ for 8 nm$<m<$ 256 nm, as shown in Fig. 2f. This means that, in this length scale, the landscape of the valley is almost memoryless, without the inherent characteristic length scale. Furthermore, the measured fractal dimension $D_f = 1.48$, which exposes the *significant* fractal nature of fracture surfaces along the valley.

Recently, Bouchaud et al. [31] has showed a similar fractal dimension (1.45) of mode I fracture surface of a notched Vit 1 bulk MG subjected to tension. They discovered that fracture occurs through the growth and coalescence of damage cavities; the maximum diameter of damage cavities reaches the order of millimeters. In the present work, as for the valley, the maximum length

scale is 256 nm perpendicular to the cracking direction (see Fig. 2f) and ~64 nm along the cracking direction (see Fig. 2b). These sizes are much greater than the characteristic size (usually from sub-nanometer to ~1 nm) of plastic voids due to cooperative STZs operations within shear bands [32,33]. This implies that the valley of NPC is not the consequence of STZ-type atomic cluster motions that contribute to plastic flow ahead of the crack tip. Instead, we ascribe such memoryless and fractal valley to another type of atomic cluster motion, i.e. TTZ [21]. More recently, based on neutron and x-ray diffraction experiments, Ma et al. [34] have revealed that over the medium-range order (MRO), the packing of the atomic cluster (or short-range order, SRO) are fractal with the dimension of 2.31. This value is equivalent to 1.31 if one-dimension case is considered [35]. As the fundamental carriers of "quasi-cleavage", cooperative TTZ operations are actually the short-time-scale SRO or/and MRO kinetics. We guess that the fractal nature ($D_f = 1.48$) of the valley of NPC maybe originates from this fractal packing of SROs. The increase in the fractal dimensions is due to both excess energy dissipation and different length scales. Whether such inheritance of fractal nature exists or not deserves to be studied in future.

The great change in Hurst parameters or fractal dimensions along the three characteristic directions provide further evidence for the physical picture of NPC formation in MGs. During dynamic propagation of a sharp crack, the severe stress intensification and short relaxation timescale ahead of the tip lead to sudden activation of several TTZs in the pre-formed fracture process zone [21,26]. Through sequential TTZ operations, the quasi-cleavage fracture occurs within a small distance from the crack tip, producing the fractal valley on either fracture surface. As a consequence of local quasi-cleavage, the high stress in front of the tip decays rapidly to the low background flow stress and the crack tip temporarily blunts. Subsequently, the coalescence of the local quasi-cleavage zone with the crack surface yields a longer crack via a few STZs operations between them. The coalescence site corresponds to the plastic peak part of the NPC. The extreme plastic flow results in the decrease in fractal dimension of the peak. A corrugation period including a peak and a valley therefore forms and the second cycle is set up. In other words, alternately activation of TTZs and STZs ahead of the crack tip induces the sharpening/blunting transition of crack front, which leads to the formation of the NPC. Keep in mind that the shear of randomly close-packed atoms can cause dilatation [32,36] and vice versa [37]. Thus, either TTZ or STZ does not occur alone and they are naturally coupled. In the "quasi-cleavage" fracture induced by TTZs, the plastic flow still occurs, but is less significant. This is why the Hurst parameter for the brittle valley is 0.52 (see Fig. 2f) rather than 0.5 for strictly memoryless process.

5. Conclusions

In summary, the landscapes of NPC on the dynamic fracture surface of a tough bulk MG are studied using AFM scans. The DFA method is adopted to analyze the AFM profiles along the three characteristic directions, i.e. the cracking, the peak and the valley. It is found that the fracture patterns along the first two directions are long-range correlated with inherent length scales, showing *non*-fractal or *weak*-fractal nature, respectively. However, the surface profiles along the valley are memoryless, characterized by a Hurst parameter of 0.52 and exhibiting a *significant* self-similar fractal character with the dimension of about 1.48. The existence of uncorrelated fracture surfaces with fractal feature indicates that there is indeed brittle fracture mechanism underpinned by TTZs-induced "quasi-cleavage" in MGs, except for conventional ductile fracture mechanism.

Acknowledgements

Financial support is from the NSFC (Grants Nos. 10725211, 10721202 and 10872206), the NSAF (Grant No. 10976100), the National Basic Research Program of China (Grant No. 2009CB724401) and the Key Project of Chinese Academy of Sciences (No. KJCX2-YW-M04).

References

[1] Spaepen F. Acta Metall 1975;23:615.
[2] Argon AS, Salama M. Mater Sci Eng 1976;23:219.
[3] Flores KM, Dauskardt RH. Intermetallics 2004;12:1025.
[4] Furukawa A, Tanaka H. Nat Mater 2009;8:601.
[5] Liu YH, Liu CT, Wang WH, Inoue A, Sakurai T, Chen MW. Phys Rev Lett 2009;103:065504.
[6] Spaepen F. In: Balian R, Kleman M, Poirier J, editors. Physics of defects. Amsterdam: North-Holland; 1981. p. 146–62.
[7] Argon AS. Acta Metall 1979;27:47.
[8] Johnson WL, Samwer K. Phys Rev Lett 2005;95:195501.
[9] Mayr SG. Phys Rev Lett 2006;97:195501.
[10] Harmon JS, Demetriou MD, Johnson WL, Samwer K. Phys Rev Lett 2007; 99:135502.
[11] Pampillo CA. J Mater Sci 1975;10:1194.
[12] Zhang ZF, Eckert J, Schultz L. Acta Mater 2003;51:1167.
[13] Xie S, George EP. Intermetallics 2008;16:485.
[14] Taylor GI. Proc Roy Soc (London) 1950;A201:192.
[15] Xi XK, Zhao DQ, Pan MX, Wang WH, Wu Y, Lewandowski JJ. Phys Rev Lett 2005;94:125510.
[16] Wang G, Zhao DQ, Bai HY, Pan MX, Xia AL, Han BS, et al. Phys Rev Lett 2007; 98:235501.
[17] Zhao JX, Qu RT, Wu FF, Zhang ZF, Shen BL, Stoica M, et al. J Appl Phys 2009; 105:103519.
[18] Pan DG, Zhang HF, Wang AM, Wang ZG, Hu ZQ. J Alloys Compds 2007; 438:145.
[19] Wang YT, Xi XK, Wang G, Xia XX, Wang WH. J Appl Phys 2009;106:113528.
[20] Shen J, Liang WZ, Sun JF. Appl Phys Lett 2006;89:121908.
[21] Jiang MQ, Ling Z, Meng JX, Dai LH. Philos Mag 2008;88:407.
[22] Meng JX, Ling Z, Jiang MQ, Zhang HS, Dai LH. Appl Phys Lett 2008;92:171909.
[23] Jiang F, Jiang MQ, Zhao YL, He L, Sun J., unpublished.
[24] Raghavan R, Murali P, Ramamurty U. Acta Mater 2009;57:3332.
[25] Escobedo JP, Gupta YM. J Appl Phys 2010;107:123502.
[26] Jiang MQ, Ling Z, Meng JX, Gao JB, Dai LH. Scripta Mater 2010;62:572.
[27] Peng CK, Buldyrev SV, Havlin S, Simons M, Stanley HE, Goldberger AL. Phys Rev E 1994;49:1685.
[28] Gao JB, Hu J, Tung WW, Cao YH, Sarshar N, Roychowdhury VP. Phys Rev E 2006;73:016117.
[29] Gao JB, Cao YH, Tung WW, Hu J. Multiscale analysis of complex time series: integration of chaos and random fractal theory, and beyond. New Jersey: John Wiley & Sons, Inc.; 2007.
[30] Madge SV, Wada T, Louzguine-Luzgin DV, Greer AL, Inoue A. Scripta Mater 2009;61:540.
[31] Bouchaud E, Boivin D, Pouchou JL, Bonamy D, Poon B, Ravichandran G. Europhys Lett 2008;83:66006.
[32] Li J, Spaepen F, Hufnagel TC. Philos Mag 2002;82:2623.
[33] Flores KM, Sherer E, Bharathula A, Chen H, Jean YC. Acta Mater 2007;55:3403.
[34] Ma D, Stoica AD, Wang X-L. Nat Mater 2009;8:30.
[35] Mandelbrot BB, Passoja DE, Paullay AJ. Nature 1984;308:721.
[36] Jiang MQ, Dai LH. Phys Rev B 2007;76:054204.
[37] Jiang MQ, Jiang SY, Dai LH. Chin Phys Lett 2009;26:016103.